Commun. Comput. Phys.
doi: 10.4208/cicp.OA-2017-0260

Vol. **25**, No. 2, pp. 448-460
February 2019

Effective Time Step Analysis of a Nonlinear Convex Splitting Scheme for the Cahn–Hilliard Equation

Seunggyu Lee[1] and Junseok Kim[2,*]

[1] *National Institute for Mathematical Sciences, Dajeon 34047, Republic of Korea.*
[2] *Department of Mathematics, Korea University, Seoul 02841, Republic of Korea.*

Received 21 December 2017; Accepted (in revised version) 3 January 2018

Abstract. We analyze the effective time step size of a nonlinear convex splitting scheme for the Cahn–Hilliard (CH) equation. The convex splitting scheme is unconditionally stable, which implies we can use arbitrary large time-steps and get stable numerical solutions. However, if we use a too large time-step, then we have not only discretization error but also time-step rescaling problem. In this paper, we show the time-step rescaling problem from the convex splitting scheme by comparing with a fully implicit scheme for the CH equation. We perform various test problems. The computation results confirm the time-step rescaling problem and suggest that we need to use small enough time-step sizes for the accurate computational results.

AMS subject classifications: 37M05, 65M22, 65T50

Key words: Cahn–Hilliard equation, convex splitting, effective time step, Fourier analysis.

1 Introduction

We consider the effective time step size of a nonlinear convex splitting scheme for the following Cahn–Hilliard (CH) equation [1]:

$$\phi_t(\mathbf{x},t) = \Delta[F'(\phi(\mathbf{x},t)) - \epsilon^2\Delta\phi(x,t)], \quad \mathbf{x}\in\Omega, \quad t>0, \tag{1.1}$$

$$\mathbf{n}\cdot\nabla\phi(\mathbf{x},t) = \mathbf{n}\cdot\nabla\mu(\mathbf{x},t) = 0, \quad \mathbf{x}\in\partial\Omega, \tag{1.2}$$

$$\phi(\mathbf{x},0) = \phi_0(\mathbf{x}), \quad \mathbf{x}\in\Omega, \quad t>0, \tag{1.3}$$

where $F(\phi) = 0.25(\phi^2-1)^2$, ϵ is the gradient energy coefficient, $\Omega = \prod_{i=1}^{d}(0,L_i)$, $d = 1,2,3$, and $\mathbf{n}$ is the outer normal vector. The CH equation is a phenomenological model of the process of a phase separation in a binary mixture [1]. Its physical applications have been extended to many scientific fields such as image inpainting, spinodal tumor growth

*Corresponding author. *Email addresses:* sglee89@nims.re.kr (S. Lee), cfdkim@korea.ac.kr (J. Kim)

simulation, decomposition, topology optimization, diblock copolymer, microstructures with elastic inhomogeneity, and multiphase fluid flows, see a recent review paper [15] for the relevant references. The CH equation can be derived by a gradient flow with the following total energy functional:

$$\mathcal{E}(\phi)=\int_\Omega\left(F(\phi)+\frac{\epsilon^2}{2}|\nabla\phi|^2\right)d\mathbf{x}. \tag{1.4}$$

That is,

$$\phi_t=-\text{grad}\mathcal{E}(\phi)=-\Delta\left(\frac{\delta\mathcal{E}(\phi)}{\delta\phi}\right), \tag{1.5}$$

where $\delta\mathcal{E}(\phi)/\delta\phi=F'(\phi)-\epsilon^2\Delta\phi$ is the variational derivative. For a review of the physical, mathematical, and numerical derivations of the CH equation, see a review paper [16]. Also, for the basic principles and practical applications of the CH Equation, see [15].

Because there has been no closed-form solution for the CH equation with arbitrary initial conditions, we need to resort to numerical approximations to solve the equation. The explicit Euler scheme has severe time-step restriction. Both the fully implicit and Crank–Nicolson schemes have also solvability time-step restriction. To overcome these time-step restrictions, Eyre proposed the following convex splitting method for the Cahn–Hilliard equation [9]:

$$\frac{\phi^{n+1}-\phi^n}{\Delta t}=-\Big[\text{grad}\mathcal{E}_c(\phi^{n+1})-\text{grad}\mathcal{E}_e(\phi^n)\Big], \tag{1.6}$$

where $\text{grad}\mathcal{E}(\phi)=\text{grad}\mathcal{E}_c(\phi)-\text{grad}\mathcal{E}_e(\phi)$. For the nonlinear stabilized splitting scheme, we define $\text{grad}\mathcal{E}_c(\phi)=-\Delta[(\phi^{n+1})^3-\epsilon^2\Delta\phi^{n+1}]$ and $\text{grad}\mathcal{E}_e(\phi^n)=-\Delta\phi^n$. Let us rewrite Eq. (1.6) in terms of the fully implicit Euler scheme:

$$\begin{aligned}\frac{\phi^{n+1}-\phi^n}{\Delta t}&=-\text{grad}\mathcal{E}_c(\phi^{n+1})+\text{grad}\mathcal{E}_e(\phi^{n+1})-\text{grad}\mathcal{E}_e(\phi^{n+1})+\text{grad}\mathcal{E}_e(\phi^n)\\&=-\text{grad}\mathcal{E}(\phi^{n+1})-\text{grad}\mathcal{E}_e(\phi^{n+1})+\text{grad}\mathcal{E}_e(\phi^n)\\&=-\text{grad}\mathcal{E}(\phi^{n+1})+\Delta(\phi^{n+1}-\phi^n).\end{aligned} \tag{1.7}$$

Then, the scheme (1.6) can be written as follows:

$$(1-\Delta t\Delta)\left(\frac{\phi^{n+1}-\phi^n}{\Delta t}\right)=-\text{grad}\mathcal{E}(\phi^{n+1}). \tag{1.8}$$

The main purpose of this article is to investigate a mode-dependent effective time-step of a nonlinear convex splitting scheme for the CH equation using the fully implicit Euler algorithm. The convex splitting method is the most popular numerical schemes in the phase-field method to overcome the time-step restriction [6, 20]. Furthermore, in recent years, the convex splitting numerical schemes have been extensively studied for the Cahn–Hilliard model coupled with a certain fluid such as the Cahn–Hilliard–Hele–Shaw [23], Cahn–Hilliard–Brinkman [7], Cahn–Hilliard–Navier–Stokes [8, 11] equations.

The difference between the effective and real time-steps have been reported when using the convex splitting method in the last decade [17,22]. To overcome this weakness, there have been extensive works of second order accurate convex splitting method for the CH equation [2,10,12,18,20,25] and a mode-dependent effective time step form was derived for the linear convex splitting scheme [3,4]; however, there is no analysis about the nonlinear convex splitting one in authors' knowledge.

This paper is organized as follows. In Section 2, we provide numerical analysis for the effective time step of a nonlinear convex splitting scheme for the CH equation. In Section 3, we perform computational experiments to confirm the numerical analysis. In Section 4, conclusions are given.

2 Numerical analysis

2.1 One-dimensional space

Now, we consider the spatial discretization. Let us denote the computational domain $\Omega_h=\{x_i : x_i=(i-0.5)h\}$ where $h=L/N$ is the spatial step size and N is the number of grid points. The approximation of ϕ^n on Ω_h is $\phi_i^n=\phi((i-0.5)h,n\Delta t)$. For the homogenous Neumann boundary condition, we define:

$$\phi_0^n=\phi_1^n,\ \phi_{N+1}^n=\phi_N^n. \tag{2.1}$$

The discrete Laplace operator Δ_h is defined by

$$\Delta_h\phi_i^n=\frac{\phi_{i+1}^n-2\phi_i^n+\phi_{i-1}^n}{h^2}. \tag{2.2}$$

Then, we can derive the formulation of the eigenvector and its corresponding eigenvalue for Δ_h [14], i.e., $\Delta_h\mathbf{v}_j=\lambda_j\mathbf{v}_j$, where $\mathbf{v}_j=(v_{1j},\cdots,v_{Nj})$ for $j=1,\cdots,N$, and

$$v_{ij}=\begin{cases}\sqrt{\frac{1}{N}} & \text{if } j=1,\\ \sqrt{\frac{2}{N}}\cos\frac{(2i-1)(j-1)\pi}{2N} & \text{otherwise,}\end{cases} \tag{2.3}$$

$$\lambda_j=-\frac{4}{h^2}\sin^2\frac{(j-1)\pi}{2N}. \tag{2.4}$$

Let $\mathbf{w}_j=\mathbf{v}_j/a_j=(w_{1j},\cdots,w_{Nj})$ where $a_1=\sqrt{1/n}$ and $a_j=\sqrt{2/n}$ for $j>1$. For convenience, we define

$$w_{0,j}=\cos\frac{-(j-1)\pi}{2N}=\cos\frac{(j-1)\pi}{2N}=w_{1,j}, \tag{2.5}$$

$$w_{N+1,j}=\cos\frac{(2N+1)(j-1)\pi}{2N}=\cos\frac{(2N-1)(j-1)\pi}{2N}=w_{N,j}. \tag{2.6}$$

Note that the discrete Fourier cosine series and its inverse transform are [19]

$$\phi_i^n = \sum_{j=1}^{N} \hat{\phi}_j^n \cos\frac{(2i-1)(j-1)\pi}{2N} = \sum_{j=1}^{N} \hat{\phi}_j^n w_{ij}, \tag{2.7}$$

$$\hat{\phi}_j^n = \frac{1}{N}\sum_{i=1}^{N} \phi_i^n \cos\frac{(2i-1)(j-1)\pi}{2N} = \frac{1}{N}\sum_{i=1}^{N} \phi_i^n w_{ij}, \tag{2.8}$$

where $\hat{\phi}_j^n$ is the Fourier coefficient. Then, for $i=1,\cdots,N$,

$$\begin{aligned}\frac{\phi_{i+1}^n - 2\phi_i^n + \phi_{i-1}^n}{h^2} &= \sum_{j=1}^{N} \hat{\phi}_j^n \frac{w_{i+1,j} - 2w_{ij} + w_{i-1,j}}{h^2} \\ &= \sum_{j=1}^{N} \left(\frac{1}{N}\sum_{k=1}^{N} \phi_k^n w_{kj} \right) \frac{w_{i+1,j} - 2w_{ij} + w_{i-1,j}}{h^2}.\end{aligned} \tag{2.9}$$

Here,

$$\begin{aligned} w_{kj}w_{i+1,j} &= \cos\frac{(2k-1)(j-1)\pi}{2N}\cos\frac{(2(i+1)-1)(j-1)\pi}{2N} \\ &= \cos\frac{(2k-1)(j-1)\pi}{2N}\left[\cos\frac{(2i-1)(j-1)\pi}{2N}\cos\frac{2(j-1)\pi}{2N}\right. \\ &\quad \left. -\sin\frac{(2i-1)(j-1)\pi}{2N}\sin\frac{2(j-1)\pi}{2N}\right] \\ &= \cos\frac{(2k-1)(j-1)\pi}{2N}\cos\frac{2(j-1)\pi}{2N}\cos\frac{(2i-1)(j-1)\pi}{2N} \\ &\quad -\cos\frac{(2k-1)(j-1)\pi}{2N}\sin\frac{(2i-1)(j-1)\pi}{2N}\sin\frac{2(j-1)\pi}{2N} \\ &= \frac{1}{2}\left[\cos\frac{(2(k+1)-1)(j-1)\pi}{2N} + \cos\frac{(2(k-1)-1)(j-1)\pi}{2N}\right] w_{ij} \\ &\quad + \frac{1}{2}w_{kj}\left[\cos\frac{(2i+1)(j-1)\pi}{2N} - \cos\frac{(2(i-1)-1)(j-1)\pi}{2N}\right] \\ &= \frac{1}{2}\left(w_{k+1,j} + w_{k-1,j}\right)w_{ij} + \frac{1}{2}w_{kj}\left(w_{ij} - w_{i-1,j}\right) \end{aligned} \tag{2.10}$$

and similarly

$$w_{kj}w_{i-1,j} = \frac{1}{2}\left(w_{k+1,j} + w_{k-1,j}\right)w_{ij} - \frac{1}{2}w_{kj}\left(w_{ij} - w_{i-1,j}\right). \tag{2.11}$$

Note that it also holds for $i=1$ and N using the boundary conditions (2.1), (2.5), and (2.6). Therefore, (2.9) can be rewritten as

$$\begin{aligned}\sum_{j=1}^{N}\left(\frac{1}{N}\sum_{k=1}^{N}\phi_k^n w_{kj}\right)\frac{w_{i+1,j}-2w_{ij}+w_{i-1,j}}{h^2} &= \sum_{j=1}^{N}\left(\frac{1}{N}\sum_{k=1}^{N}\phi_k^n\left(\Delta_h w_{kj}\right)\right)w_{ij}\\ &= \sum_{j=1}^{N}\lambda_j\left(\frac{1}{N}\sum_{k=1}^{N}\phi_k^n w_{kj}\right)w_{ij}\\ &= \sum_{j=1}^{N}\lambda_j\hat{\phi}_j^n w_{ij}. \end{aligned} \tag{2.12}$$

Then,

$$(1-\Delta t\Delta_h)\left(\frac{\phi_i^{n+1}-\phi_i^n}{\Delta t}\right)=\sum_{j=1}^{N}(1-\Delta t\lambda_j)\left(\frac{\hat{\phi}_j^{n+1}-\hat{\phi}_j^n}{\Delta t}\right)w_{ij}. \tag{2.13}$$

Moreover, the scheme (1.8) can be rewritten as follows:

$$\sum_{j=1}^{N}(1-\Delta t\lambda_j)\left(\frac{\hat{\phi}_j^{n+1}-\hat{\phi}_j^n}{\Delta t}\right)w_{ij}=-\sum_{j=1}^{N}\mathcal{F}\left(\text{grad}\mathcal{E}\left(\phi^{n+1}\right)\right)w_{ij}, \tag{2.14}$$

where $\mathcal{F}(\cdot)$ represents the fourier coefficient. Hence, the mode-dependent effective time step Δt_e is

$$\Delta t_e=\frac{\Delta t}{1-\lambda_j\Delta t}, \tag{2.15}$$

for each basis $\mathbf{w}_j$ in the Fourier space.

2.2 Two-dimensional space

The analysis of a mode-dependent effective time step based on the eigenfunction decomposition and eigenvalue estimation can be extended to the two- and three-dimensional spaces. Here, we present the analysis only for the two-dimensional space since it is similar enough to extend to the three-dimensional space straightforwardly. First, similar to the one-dimensional space, we define the computational domain $\Omega_h=\{x_i,y_j : x_i=(i-0.5)h,\ y_j=(j-0.5)h\}$ where $h=L_1/N_x=L_2/N_y$ is the uniform spatial step size, N_x and N_y are the number of grid points in x- and y-directions, respectively, and the approximation of ϕ^n on Ω_h is $\phi_{ij}^n=\phi((i-0.5)h,(j-0.5)h,n\Delta t)$. For the homogenous Neumann boundary condition, we define:

$$\phi_{i,0}^n=\phi_{i,1}^n,\quad \phi_{i,N_y+1}^n=\phi_{i,N_y}^n \quad \text{for } i=1,\cdots,N_x, \tag{2.16}$$

$$\phi_{0,j}^n=\phi_{1,j}^n,\quad \phi_{N_x+1,j}^n=\phi_{N_x,j}^n \quad \text{for } j=1,\cdots,N_y. \tag{2.17}$$

The discrete Laplace operator Δ_h for the two-dimensional space is defined by

$$\Delta_h \phi_{ij}^n = \frac{\phi_{i+1,j}^n + \phi_{i-1,j}^n - 4\phi_{ij}^n + \phi_{i,j+1}^n + \phi_{i,j-1}^n}{h^2}. \tag{2.18}$$

Note that the eigenvector and its corresponding eigenvalue for (2.18) can be derived using the Kronecker (tensor) product (Refer to [13]). If we denote the element of tensor product $\mathbf{v}_i \otimes \mathbf{v}_j$ as $v_{ik\otimes jl}$, the formulation of the eigenvector and the eigenvalues are

$$v_{ik\otimes jl} = v_{ik} v_{jl} = \begin{cases} \sqrt{\frac{1}{N_x N_y}} & \text{if } k=1 \text{ and } l=1, \\ \sqrt{\frac{2}{N_x N_y}} \cos\frac{(2i-1)(k-1)\pi}{2N_x} & \text{if } k>1 \text{ and } l=1, \\ \sqrt{\frac{2}{N_x N_y}} \cos\frac{(2j-1)(l-1)\pi}{2N_y} & \text{if } k=1 \text{ and } l>1, \\ \sqrt{\frac{4}{N_x N_y}} \cos\frac{(2i-1)(k-1)\pi}{2N_x} \cos\frac{(2j-1)(l-1)\pi}{2N_y} & \text{otherwise,} \end{cases} \tag{2.19}$$

$$\lambda_{kl} = \lambda_k + \lambda_l = -\frac{4}{h^2}\left[\sin^2\frac{(k-1)\pi}{2N_x} + \sin^2\frac{(l-1)\pi}{2N_y}\right]. \tag{2.20}$$

Recall that the discrete Fourier cosine series and its inverse transform are

$$\phi_{ij}^n = \sum_{k=1}^{N_x}\sum_{l=1}^{N_y} \hat{\phi}_{kl}^n w_{ik\otimes jl}, \quad \hat{\phi}_{kl}^n = \frac{1}{N_x N_y}\sum_{i=1}^{N_x}\sum_{j=1}^{N_y} \phi_{ij}^n w_{ik\otimes jl}. \tag{2.21}$$

Since

$$\frac{\phi_{i+1,j}^n + \phi_{i-1,j}^n - 4\phi_{ij}^n + \phi_{i,j+1}^n + \phi_{i,j-1}^n}{h^2} = \frac{\phi_{i+1,j}^n - 2\phi_{ij}^n + \phi_{i-1,j}^n}{h^2} + \frac{\phi_{i,j+1}^n - 2\phi_{ij}^n + \phi_{i,j-1}^n}{h^2}, \tag{2.22}$$

we can apply Eqs. (2.9), (2.10), and (2.11) into each terms. Then, for $i=1,\cdots,N_x$ and $j=1,\cdots,N_y$,

$$\begin{aligned} \Delta_h \phi_{ij}^n &= \sum_{k=1}^{N_x}\sum_{l=1}^{N_y}\left(\frac{1}{N_x N_y}\sum_{p=1}^{N_x}\sum_{q=1}^{N_y}\phi_{pq}^n w_{pk} w_{ql}\right)\frac{w_{i+1,k} - 2w_{ik} + w_{i-1,k}}{h^2} w_{jl} \\ &\quad + \sum_{k=1}^{N_x}\sum_{l=1}^{N_y}\left(\frac{1}{N_x N_y}\sum_{p=1}^{N_x}\sum_{q=1}^{N_y}\phi_{pq}^n w_{pk} w_{ql}\right) w_{ik}\frac{w_{j+1,l} - 2w_{jl} + w_{j-1,l}}{h^2} \\ &= \sum_{k=1}^{N_x}\sum_{l=1}^{N_y}\left(\frac{1}{N_x N_y}\sum_{p=1}^{N_x}\sum_{q=1}^{N_y}\phi_{pq}^n \frac{w_{p+1,k} - 2w_{pk} + w_{p-1,k}}{h^2} w_{ql}\right) w_{ik} w_{jl} \\ &\quad + \sum_{k=1}^{N_x}\sum_{l=1}^{N_y}\left(\frac{1}{N_x N_y}\sum_{p=1}^{N_x}\sum_{q=1}^{N_y}\phi_{pq}^n w_{pk}\frac{w_{q+1,l} - 2w_{ql} + w_{q-1,l}}{h^2}\right) w_{ik} w_{jl} \\ &= \sum_{k=1}^{N_x}\sum_{l=1}^{N_y}\left(\frac{1}{N_x N_y}\sum_{p=1}^{N_x}\sum_{q=1}^{N_y}\phi_{pq}^n \Delta_h w_{pk\otimes ql}\right) w_{ik} w_{jl} = \sum_{k=1}^{N_x}\sum_{l=1}^{N_y}\lambda_{kl}\hat{\phi}_{kl}^n w_{ik\otimes jl}. \end{aligned} \tag{2.23}$$

Similar to Eqs. (2.13) and (2.14), we can calculate the mode-dependent effective time step Δt_e in a two-dimensional space as follows:

$$\Delta t_e = \frac{\Delta t}{1-\lambda_{jk}\Delta t}, \tag{2.24}$$

for each basis $\mathbf{w}_j \otimes \mathbf{w}_k$ in the Fourier space.

In this paper, we study a mode-dependent effective time step of a nonlinear convex splitting scheme (2.25) for the CH equation using the fully implicit Euler algorithm (2.26): for $i=1,\cdots,N_x$ and $j=1,\cdots,N_y$

$$\frac{\phi_{ij}^{n+1}-\phi_{ij}^{n}}{\Delta t} = \Delta_h[(\phi_{ij}^{n+1})^3 - \phi_{ij}^{n} - \epsilon^2\Delta_h\phi_{ij}^{n+1}], \tag{2.25}$$

$$\frac{\phi_{ij}^{n+1}-\phi_{ij}^{n}}{\Delta t} = \Delta_h[(\phi_{ij}^{n+1})^3 - \phi_{ij}^{n+1} - \epsilon^2\Delta_h\phi_{ij}^{n+1}]. \tag{2.26}$$

3 Computational results

3.1 One-dimensional cases

If we choose $\epsilon=\epsilon_m = mh/[2\sqrt{2}\tanh^{-1}(0.9)]$, then we have approximately mh transition layer across interface [5]. Unless otherwise specified, we use $N=128$, $h=1/N$, and $\epsilon=\epsilon_6$. For the numerical solution algorithm, we use a nonlinear multigrid method [21,24].

Fig. 1 plots eigenvalues $\lambda_j = -\frac{4}{h^2}\sin^2\frac{(j-1)\pi}{2N}$ for $j=1,\cdots,N$. The values are monotonically decreasing.

Fig. 2 shows the effective time step $\Delta t_e = \Delta t/(1-\lambda_j\Delta t)$ for three different time steps $\Delta t = 2h^2$, $0.2h^2$, $0.02h^2$, where $\lambda_j = -\frac{4}{h^2}\sin^2\frac{(j-1)\pi}{2N}$ for $j=1,\cdots,N$. The result indicates that the effect time step varies with large scale as the time step size increases.

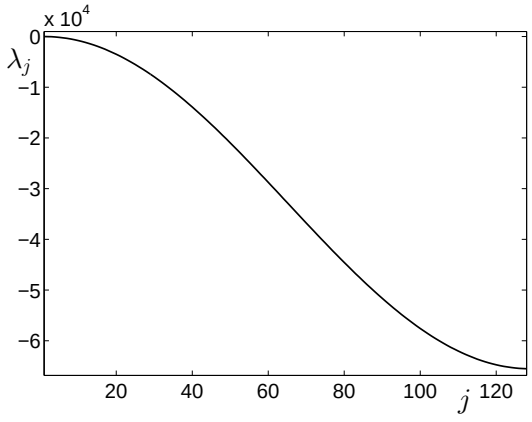

Figure 1: Plot of eigenvalues $\lambda_j = -\frac{4}{h^2}\sin^2\frac{(j-1)\pi}{2N}$ for $i=1,\cdots,N$.

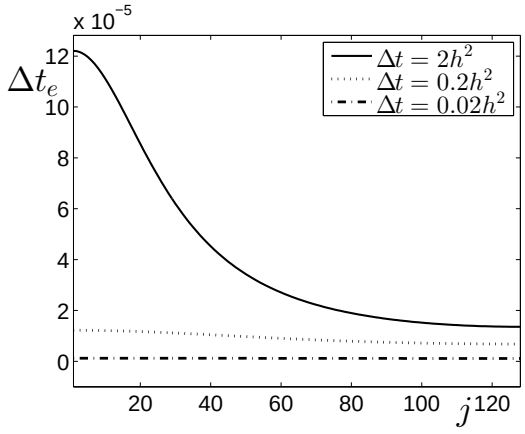

Figure 2: The effective time step $\Delta t_e = \Delta t/(1-\lambda_j \Delta t)$ for three different $\Delta t = 2h^2$, $0.2h^2$, $0.02h^2$, where $\lambda_j = -\frac{4}{h^2}\sin^2\frac{(j-1)\pi}{2N}$ for $i = 1,\cdots,N$.

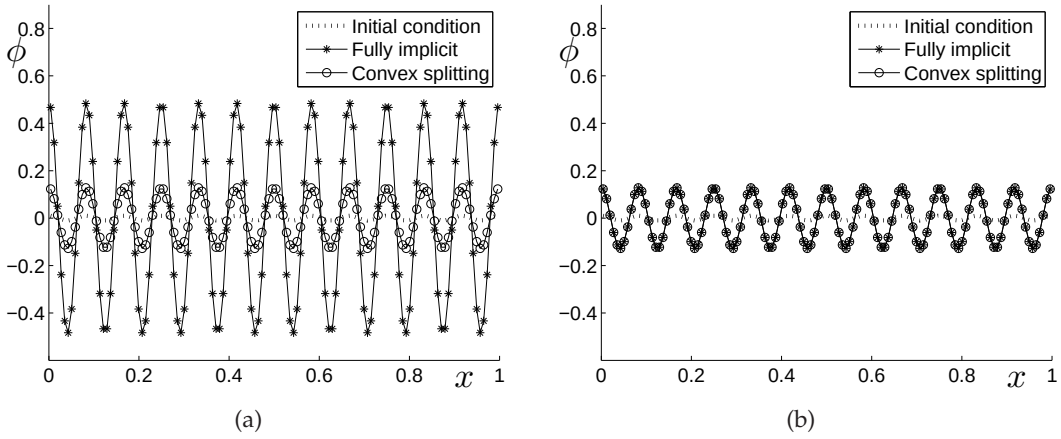

Figure 3: Initial condition is $\phi(x,0) = 0.01\cos(24\pi x)$ on $\Omega = (0,1)$. Results after 20 time step iterations: (a) $\Delta t = 2h^2$ for both the schemes. (b) $\Delta t = 2h^2$ for the convex scheme and $\Delta t_e = \Delta t/(1-\lambda_{25}\Delta t)$ for the fully implicit scheme.

Let us consider an initial condition: $\phi(x,0) = 0.01\cos(24\pi x)$ on $\Omega = (0,1)$, which implies $j = 25$ is used. Fig. 3 shows the results after 20 time step iterations: (a) $\Delta t = 2h^2$ is used for both the schemes. We can observe time delay for the nonlinear convex splitting scheme compared to the fully implicit Euler scheme. (b) $\Delta t = 2h^2$ is used for the convex scheme and $\Delta t_e = \Delta t/(1-\lambda_{25}\Delta t)$ is used for the fully implicit scheme. The results from the two different schemes are almost identical.

Next, we consider a high-frequency mode, i.e., a damping mode: $\phi(x,0) = 0.3\cos(34\pi x)$. Fig. 3(a) shows the results after 5 time step iterations with $\Delta t = 2h^2$ for both the schemes. Similar to the previous test, we can observe time delay for the nonlinear convex splitting

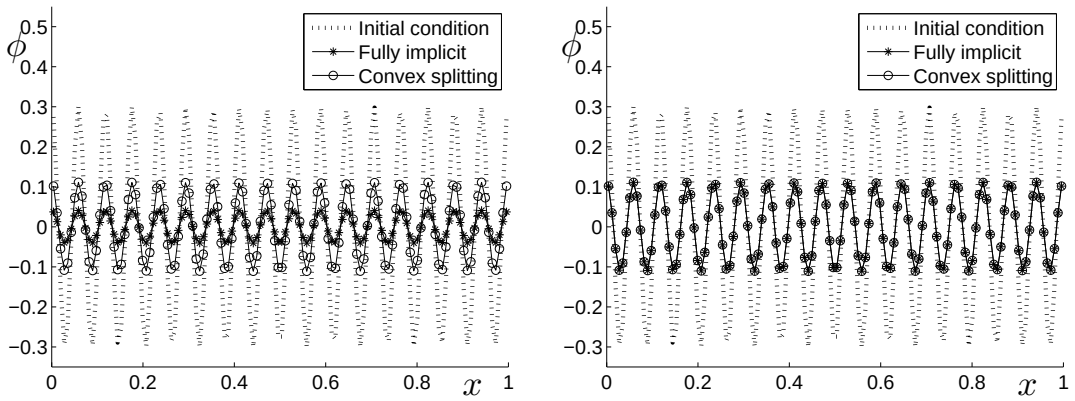

Figure 4: Initial condition is $\phi(x,0)=0.3\cos(34\pi x)$ on $\Omega=(0,1)$. Results after 5 time step iterations: (a) $\Delta t=2h^2$ for both the schemes. (b) $\Delta t=2h^2$ for the convex scheme and $\Delta t_e=\Delta t/(1-\lambda_{35}\Delta t)$ for the fully implicit scheme.

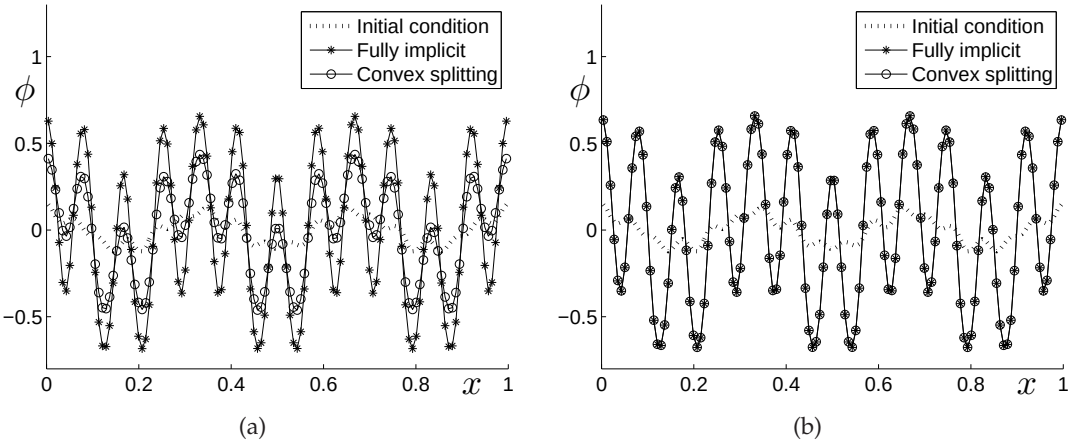

Figure 5: Initial condition is $\phi(x,0)=0.03\cos(34\pi x)+0.02\cos(24\pi x)+0.1\cos(6\pi x)$. (a) Snapshot at $T=25\Delta t$, where $\Delta t=2h^2$. (b) Snapshot at $T=2500\Delta t$, where $\Delta t=0.02h^2$.

scheme. Fig. 3(b) shows a good agreement between the two results with $\Delta t=2h^2$ for the convex scheme and $\Delta t_e=\Delta t/(1-\lambda_{35}\Delta t)$ for the fully implicit scheme.

Fig. 5 shows snapshots of the profiles using two schemes and two time steps. The initial condition is $\phi(x,0)=0.03\cos(34\pi x)+0.02\cos(24\pi x)+0.1\cos(6\pi x)$. If we use a large time step ($\Delta t=2h^2$), then due to the time step re-scaling there is delay of the temporal evolution for the nonlinear splitting scheme compared to the fully implicit scheme (see Fig. 5(a)). However, if we use a small enough time step ($\Delta t=0.02h^2$), then we can observe the agreement between two results as shown in Fig. 5(b).

3.2 Two-dimensional space

Fig. 6 plots eigenvalues $\lambda_{kl}=\lambda_k+\lambda_l=-\frac{4}{h^2}\left[\sin^2\frac{(k-1)\pi}{2N_x}+\sin^2\frac{(l-1)\pi}{2N_y}\right]$ for $k=1,\cdots,N_x$ and $l=1,\cdots,N_y$.

Figs. 7(a), (b), and (c) show the effective time step $\Delta t_e=\Delta t/(1-\lambda_{kl}\Delta t)$ for three different $\Delta t=h^2$, $0.2h^2$, $0.02h^2$, respectively, where $\lambda_{kl}=\lambda_k+\lambda_l=-\frac{4}{h^2}\left[\sin^2\frac{(k-1)\pi}{2N_x}+\sin^2\frac{(l-1)\pi}{2N_y}\right]$ for $k=1,\cdots,N_x$ and $l=1,\cdots,N_y$. The result indicates that the effect time step varies with large scale as the time step size increases.

Let us consider an initial condition: $\phi(x,y,0)=0.01\cos(20\pi x)\cos(20\pi y)$ on $\Omega=(0,1)\times(0,1)$, which implies $k=l=21$ is used. Figs. 8(a), (b), and (c) show the initial condition, results after 200 time step iterations with $\Delta t=h^2$ for the implicit and the convex splitting schemes, respectively. Fig. 8(d) is the difference between the results from the convex scheme with $\Delta t=h^2$ and the fully implicit scheme with $\Delta t_e=\Delta t/(1-\lambda_{21,21}\Delta t)$, which implies that the results from the two different schemes with the two different time step sizes are almost identical. We can observe time delay for the nonlinear convex splitting scheme compared to the fully implicit Euler scheme.

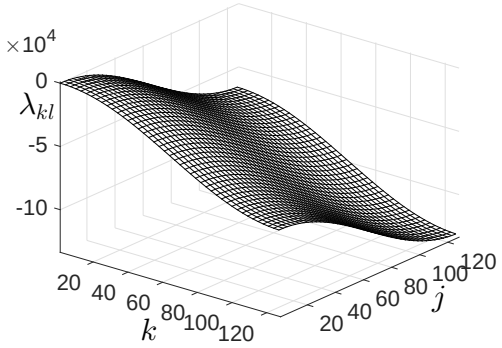

Figure 6: Plot of eigenvalues $\lambda_{kl}=\lambda_k+\lambda_l=-\frac{4}{h^2}\left[\sin^2\frac{(k-1)\pi}{2N_x}+\sin^2\frac{(l-1)\pi}{2N_y}\right]$ for $k=1,\cdots,N_x$ and $l=1,\cdots,N_y$.

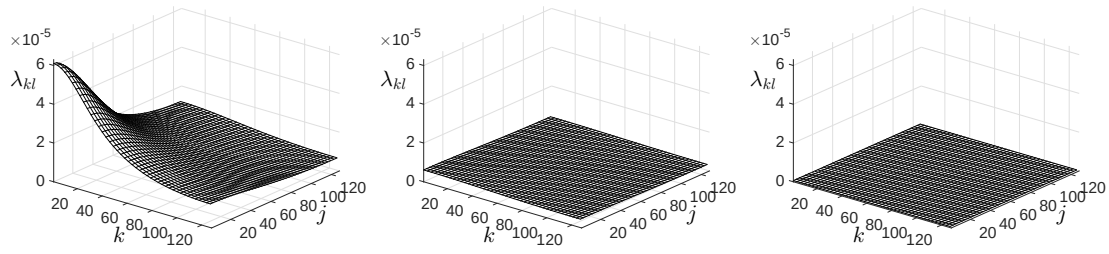

Figure 7: (a), (b), and (c) are the effective time step $\Delta t_e=\Delta t/(1-\lambda_{kl}\Delta t)$ for three different $\Delta t=h^2$, $0.1h^2$, $0.01h^2$, respectively, where $\lambda_{kl}=\lambda_k+\lambda_l=-\frac{4}{h^2}\left[\sin^2\frac{(k-1)\pi}{2N_x}+\sin^2\frac{(l-1)\pi}{2N_y}\right]$ for $k=1,\cdots,N_x$ and $l=1,\cdots,N_y$.

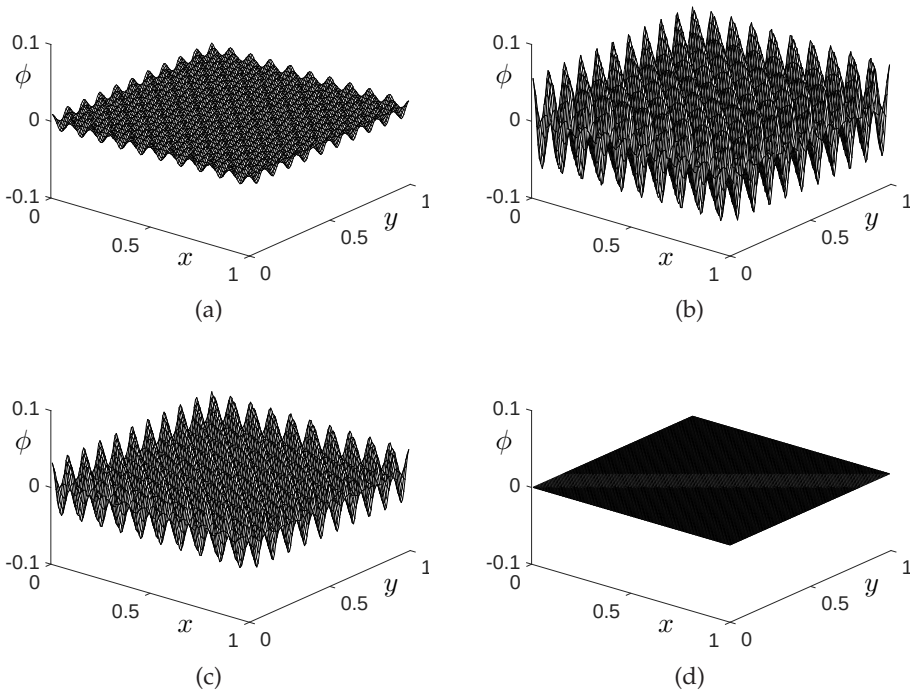

Figure 8: (a) is the initial condition, $\phi(x,y,0)=0.01\cos(20\pi x)\cos(20\pi y)$ on $\Omega=(0,1)\times(0,1)$. (b) and (c) are results after 200 time step iterations with $\Delta t=h^2$ for the implicit and the convex splitting schemes, respectively. (d) is the difference between the results from the convex scheme with $\Delta t=h^2$ and the fully implicit scheme with $\Delta t_e=\Delta t/(1-\lambda_{21,21}\Delta t)$.

Next, let us consider an initial condition: $\phi(x,y,0)=0.3\cos(30\pi x)\cos(30\pi y)$ on $\Omega=(0,1)\times(0,1)$, which implies $k=l=31$ is used. Figs. 9(a), (b), and (c) show the initial condition, results after 200 time step iterations with $\Delta t=h^2$ for the implicit and the convex splitting schemes, respectively. Fig. 9(d) is the difference between the results from the convex scheme with $\Delta t=h^2$ and the fully implicit scheme with $\Delta t_e=\Delta t/(1-\lambda_{21,21}\Delta t)$, which demonstrates that the results from the two different methods with the two different time step sizes are almost identical. We can observe time delay for the nonlinear convex splitting method compared to the fully implicit Euler method.

4 Conclusion

We investigated the effective time step size of a nonlinear convex splitting scheme for the CH equation by comparing with the fully implicit Euler method. Although the nonlinear convex splitting scheme is unconditionally stable, we need to use a small enough time step to get an accurate numerical solution. As future research, it would be practical to extend current study to the three-dimensional CH equation.

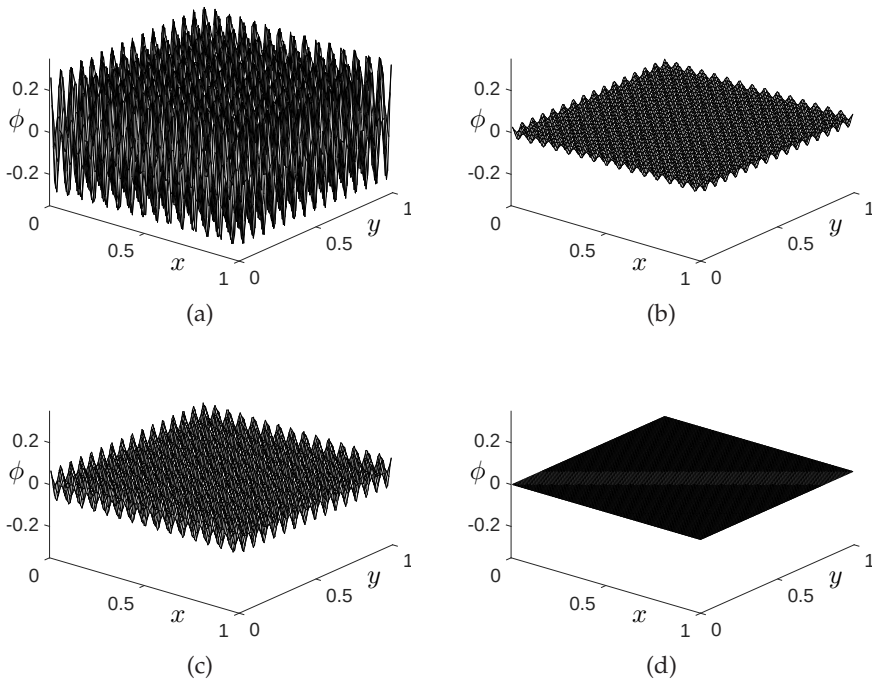

Figure 9: (a) is the initial condition, $\phi(x,y,0)=0.3\cos(30\pi x)\cos(30\pi y)$ on $\Omega=(0,1)\times(0,1)$. (b) and (c) are results after 200 time step iterations with $\Delta t=h^2$ for the implicit and the convex splitting schemes, respectively. (d) is the difference between the results from the convex scheme with $\Delta t=h^2$ and the fully implicit scheme with $\Delta t_e=\Delta t/(1-\lambda_{31,31}\Delta t)$.

Acknowledgments

The first author (S. Lee) was supported by the National Institute for Mathematical Sciences (NIMS) grant funded by the Korean government (No. A21300000) and the National Research Foundation of Korea (NRF) grant funded by the Korea government(MSIP) (No. 2017R1C1B1001937). The corresponding author (J. Kim) was supported by Basic Science Research Program through the National Research Foundation of Korea (NRF) funded by the Ministry of Education (NRF-2016R1D1A1B03933243). The authors thank the reviewers for the constructive and helpful comments on the revision of this article.

References

[1] J. Cahn and J. Hilliard, Spinodal decomposition: A reprise, Acta Metall. 19:151–161, 1971.
[2] K. Cheng, C. Wang, S.M. Wise, X. Yue, A second-order, weakly energy-stable pesudo-spectral scheme for the Cahn–Hilliard equation and its solution by the hogomenous linear iterations method, J. Sci. Comput. 69:1083–1114, 2016.
[3] M. Cheng and D. Rutenberg, Maximally fast coarsening algorithms, Phys. Rev. E 72:055701, 2005.

[4] M. Cheng, J. A. Warren, Controlling the accuracy of unconditionally stable algorithms in the Cahn–Hilliard equation, Phys. Rev. E 75:017702, 2007.
[5] J. Choi, H. Lee, D. Jeong, and J. Kim, An unconditionally gradient stable numerical method for solving the Allen–Cahn equation, Physica A 388:1791–1803, 2009.
[6] D.A. Cogswell and M.L. Szulczewski, Simulation of incompressible two-phase flow in porous media with large timesteps, J. Comput. Phys 345:856–865, 2017.
[7] C. Collins, J. Shen, S.M. Wise, An efficient, energy stable scheme for the Cahn–Hilliard–Brinkman system, Commun. Comput. Phys. 13.4:929–957, 2013.
[8] S. Engblom, M. Do-Quang, G. Amberg, A. Tornberg, On diffuse interface modeling and simulation of surfactants in two-phase fluid flow, Commun. Comput. Phys. 14.4:879–915, 2013.
[9] D. Eyre, An unconditionally stable one-step scheme for gradient systems, preprint (1997) http://www.math.utah.edu/∼eyre/research/methods/stable.ps
[10] X. Feng, T. Tang, J. Yang, Long time numerical simulations for phase-field problems using p-adaptive spectral deferred correction methods, SIAM J. Sci. Comput. 37.1:A271–A294, 2015.
[11] G. Grün, F. Gullén-González, S. Metzger, On fully decoupled, convergent scheme for diffuse interface models for two-phase flow with general mass densities, Commun. Comput. Phys. 19.5:1473–1502, 2016.
[12] J. Guo, C. Wang, S.M. Wise, X. Yue, An H^2 convergence of a second-order convex-splitting, finite difference scheme for the three-dimensional Cahn–Hilliard equation, Commun. Math. Sci. 14.2:489–515, 2016.
[13] W. Hackbusch, B.N. Khoromskij, S. Sauter, E.E. Tyrtyshnikov, Use of tenfor formats in Elliptic eigenvalue problems, Numer. Linear Algebr. 19.1:133–151, 2012.
[14] F. Hildebrand, Finite difference equations and simulations, Prentice-Hall: Englewood Cliffs, 1968.
[15] J. Kim, S. Lee, Y. Choi, S. Lee, D. Jeong, Basic principles and practical applications of the Cahn–Hilliard equation, Math. Probl. Eng. 2016:9532608, 2016.
[16] D. Lee, J. Huh, D. Jeong, J. Shin, A. Yun, and J. Kim, Physical, mathematical, and numerical derivations of the Cahn–Hilliard equation, Comput. Mater. Sci. 81:216–225, 2014.
[17] S. Lee, C. Lee, H. G. Lee, and J. Kim, Comparison of different numerical schemes for the Cahn-Hilliard equation, J. KSIAM 17:197–207, 2013.
[18] F. Luo, T. Tang, H. Xie, Parameter-free time adaptivity based on energy evolution for the Cahn–Hilliard equation, Commun. Comput. Phys. 19.5:1542–1563, 2016.
[19] W. Press, S. Teukolsky, W. Vetterling, and B. Flannery, Numerical Recipes: The Art of Scientific Computing, Cambridge University Press, 3rd ed., 2007.
[20] J. Shin, H.G. Lee, and J.-Y. Lee, Unconditionally stable methods for gradient flow using Convex Splitting RungeKutta scheme, J. Comput. Phys. 347:367–381, 2017.
[21] U. Trottenberg, C. Oosterlee, and A. Schuller, Multigrid, Academic Press, 2002.
[22] S. Wise, C. Wang, and S. Lowengrub, An energy-stable and convergent finite-difference scheme for the phase field crystal equation, SIAM J. Numer. Anal 47.3:2269–2288, 2009.
[23] S. Wise, Unconditionally stable finite difference, nonlinear, multigrid simulation of the Cahn–Hilliard–Hele–Shaw system of equations, J. Sci. Comput. 44.1:38–68, 2010.
[24] S.-D. Yang, H. G. and Lee, J. Kim, A phase-field approach for minimizing the area of triply periodic surfaces with volume constraint, Comput. Phys. Commun. 181:1037–1046, 2010.
[25] Z.R. Zhang, Z.H. Qiao, An adaptive time-stepping strategy for the Cahn–Hilliard equation, Commun. Comput. Phys. 11:1261–1278, 2012.